Science of the Total Environment 407 (2009) 3004–3016

Contents lists available at ScienceDirect

Science of the Total Environment

journal homepage: www.elsevier.com/locate/scitotenv

An advanced modelling tool for simulating complex river systems

Ana Rosa Trancoso [a,*], Frank Braunschweig [b], Pedro Chambel Leitão [a], Matthias Obermann [c], Ramiro Neves [a]

[a] MARETEC, Technical Superior Institute, Lisbon Technical University-Av. Rovisco Pais 1049-001 Lisboa, Portugal
[b] Action Modulers, Rua Cidade de Frehel, Bloco B, n°12[a], 2640-469 Mafra, Portugal
[c] Division of Water Resources Management, Institute for Water Quality and Waste Management (ISAH), Leibniz Universität Hannover, Am kleinen Felde 30, 30167 Hannover, Germany

ARTICLE INFO

Article history:
Received 30 June 2008
Received in revised form 31 December 2008
Accepted 6 January 2009
Available online 12 February 2009

Keywords:
Modelling
River network
Water quality
Object oriented programming

ABSTRACT

The present paper describes MOHID River Network (MRN), a 1D hydrodynamic model for river networks as part of MOHID Water Modelling System, which is a modular system for the simulation of water bodies (hydrodynamics and water constituents). MRN is capable of simulating water quality in the aquatic and benthic phase and its development was especially focused on the reproduction of processes occurring in temporary river networks (flush events, pools formation, and transmission losses). Further, unlike many other models, it allows the quantification of settled materials at the channel bed also over periods when the river falls dry. These features are very important to secure mass conservation in highly varying flows of temporary rivers. The water quality models existing in MOHID are base on well-known ecological models, such as WASP and ERSEM, the latter allowing explicit parameterization of C, N, P, Si, and O cycles. MRN can be coupled to the basin model, MOHID Land, with computes runoff and porous media transport, allowing for the dynamic exchange of water and materials between the river and surroundings, or it can be used as a standalone model, receiving discharges at any specified nodes (ASCII files of time series with arbitrary time step). These features account for spatial gradients in precipitation which can be significant in Mediterranean-like basins. An interface has been already developed for SWAT basin model.

© 2009 Elsevier B.V. All rights reserved.

1. Introduction

Modelling of water flow and transport processes are, nowadays, common tasks for research, planning and monitoring activities. The research and management advantages of a model increase with interdisciplinary integration. MOHID is an integrated modelling system maintained and developed by the MARETEC (Marine and Environmental Technology Research Centre) group of Technical Superior Institute at the Technical University of Lisbon (www.mohid.com). Its range of applicability has been continuously widened. It was initially developed to simulate the flow in estuarine and coastal waters (Neves, 1985) and then extended to include water quality and sediment transport processes. In 2000, the system was reorganised to be able to simulate the flow using general coordinates (Martins et al., 2001) and in any type of environment, such as groundwater, basins and river networks, due to its modularity and object oriented structure (Miranda et al., 2000; Braunschweig et al., 2004). Since then, it has been constantly enhanced by additional features and modules. Currently, MOHID is a water modelling system that can simulate 1D river networks to 2D basins and 3D estuarine and coastal waters and soil processes.

MOHID has been used in several Portuguese estuaries to simulate transport processes, sediment dynamics and water quality (Cancino and Neves, 1999b; Pina et al., 2003; Trancoso et al., 2005; Saraiva et al., 2007). It has also been applied to ocean circulation (Santos et al., 2002; Coelho and Santos, 2003) and to oil spill modelling (Montero et al., 2003).

The present paper describes MOHID River Network (MRN), which arose from the necessity of having improved inland boundary conditions for the estuary and coastal waters models, and to help manage environmental problems posed by interior waters. From its earlier development stages, MRN took into consideration the need to simulate basins which can be classified as semi-arid, and are characterised by:

(a) long periods with a partial or complete dry river network,
(b) pools formation in river transects where water remains even after surface flow has ceased,
(c) intense flush events resulting from typical Mediterranean storms, and
(d) transmission losses due to permeable river beds and soils (infiltration) and high temperatures in summer (evaporation).

Modelling these semi-arid basins and, more generally, temporary waters, poses a numerical challenge due to the high spatial and temporal gradients and proximity of zero value. These conditions are not well handled or not simulated at all in most of the currently

* Corresponding author. Tel.: +351 218 419 440; fax: +351 218 417 365.
E-mail address: arosa@ist.utl.pt (A.R. Trancoso).

0048-9697/$ – see front matter © 2009 Elsevier B.V. All rights reserved.
doi:10.1016/j.scitotenv.2009.01.015

available watershed models, as reviewed in, for example, Borah and Bera (2004) or Kalin and Hantush (2006). The widely-used SWAT model (Arnold et al., 1998) allows the user to include pools. Transmission losses are also accommodated, but since SWAT uses a daily and monthly time step, it is not suitable to simulate the extreme flush events of interest in temporary waters. HSPF (Bicknell et al., 1993) uses a coarse routing approach and does not allow time steps shorter than 1 hour. It also does not allow pools and transmission losses to be simulated. All models classified by Borah and Bera (2004) as "Single Event", such as MIKE SHE (Refsgaard and Storm, 1995), have a time step controlled by numerical stability, making them suitable for describing flush events. Of these models, only KINEROS (Woolhiser et al., 1990) allows the inclusion of pools. These examples demonstrate some of the limitations of existing models.

MOHID River Network (MRN) is a hydrodynamic model that considers a network of tributaries and allows for dynamic time step. It can also compute properties transport, such as nutrients and sediments. Being part of the general MOHID framework, it can use the 0D water quality models included in MOHID. MRN can compute water storage in pools, transmission losses and evaporation fluxes with the fine spatial and temporal discretisation required by temporary waters.

It was developed as a companion module of the basin model MOHID Land (Braunschweig et al., 2004) in order to allow dynamic exchange of water and material carried between the river and the river banks. In normal conditions runoff carries material (i.e. water, sediment, nutrients etc) to the river and during floods the river exports material across the river bank onto adjacent floodplain areas when the level of the water inside the river channels exceeds full bank storage. MRN can however be used independently of MOHID Land, as a standalone model. In that case this module imports results of the basin as point sources in the format of time series.

In MOHID Land, different processes occurring in a basin are programmed in different modules, allowing simulation of the desired ones only. The processes simulated, depicted in Fig. 1, can be 2D overland flow, 1D drainage network transport, and 3D infiltration and saturated and unsaturated porous media transport.

Due to this structure, MRN can be used as a standalone model, importing basin material as point sources in the format of time series, or integrated into MOHID Land where the interactions between the different processes (e.g. water exchange between aquifer and MRN) are calculated dynamically by the model, using hydraulic gradients. In this case, each node in the drainage network corresponds to a cell in the grid used by the other compartments, where there is flow exchange.

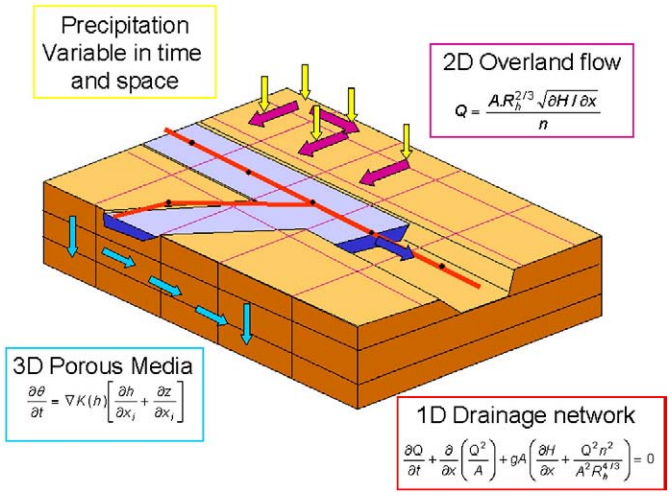

Fig. 1. Schematic representation of MOHID Land modules for hydrodynamic calculus.

MOHID Land was developed within three EU projects: EcoRiver, TempQsim and ICReW for the simulation of water flow in watersheds with pathways for river and groundwater flow. Porous media module was developed in close collaboration with soil scientists from EAN-INIA (Portuguese National Agronomic Station).

This paper begins with a description of MRN model (Section 2) presenting its main equations (Section 2.1) and how they are handled by the model (Sections 2.2 and 2.3), specific processes formulation, such as water quality, sediment dynamics, pools and transmission losses along river channels, and coupling to run-off models (Sections 2.4 to 2.7). Next, verification examples are presented in a schematic river and in a real long term simulation of the Trancão basin (Section 3), followed by the main conclusions (Section 4).

2. MRN model description

2.1. General description of MOHID

The MOHID Water Modelling System (www.mohid.com) has been constructed using an object oriented approach to facilitate integration of new processes and models. The numerical algorithms are based on the finite volume approach, a flux-driven strategy that facilitates the coupling of different processes and allows conservation of mass and momentum.

MOHID is programmed in ANSI FORTRAN 95, a language where object creation is not achieved by class instantiation but through module instantiation (Braunschweig et al., 2004). Since the start of MOHID, more than 72 modules with over 300 k codes lines have been written. Further developments can take advantage of these existing modules, limiting the requirements for new coding. The hierarchical structure of the MOHID framework is presented in Fig. 2. The lower level models (Base 1) are grid independent (i.e., 0D or 1D) and produce the MRN and Water Quality models (executables in the figure). The Base 2 modules are grid dependent and produce among others, MOHID Surface water model, which can be 2D or 3D, and MOHID Land, which is 2D for runoff and 3D for porous media processes.

MOHID I/O formats are in the form of time series at a given point (ASCII files) and/or matrix data in HDF5 binary format. There are several tools to produce, convert to and from, and to visualize these files, such as MOHID GIS and MOHID GUI (Braunschweig et al., 2005). These interfaces can use the Triangulation, TidePreview and Digital-TerrainCreator executables in Fig. 2.

In the case of MRN, the model needs an ASCII file of the drainage network, time series of arbitrary time step of solar radiation, air temperature, cloud cover, relative humidity and wind speed for the run period. The drainage network consists of nodes and reaches and can be constructed from the digital elevation model with MOHID GIS. Point discharges, pools and time series outputs can be specified along the network. For every point discharge, flow, temperature or constituents can be either constant or given as external time series. Variables initialization and needed parameters (e.g., growth rates, half saturation constants) for the sub models can be either specified in ASCII files by keyword/value pairs or left to the default value preset in the model.

The next sections describe the equations solved by the MRN to model fluid flow (continuity and momentum) and the fate of water constituents, by means of transport, reactions with other constituents (water quality processes), erosion and deposition to river beds and accumulation in pools.

2.2. Governing equations of MRN

Fluid flow is governed by conservation equations for mass, momentum, energy and any additional constituents. The numerical algorithm is based on the finite volume approach and for that reason equations are presented in their integral form. Following this strategy

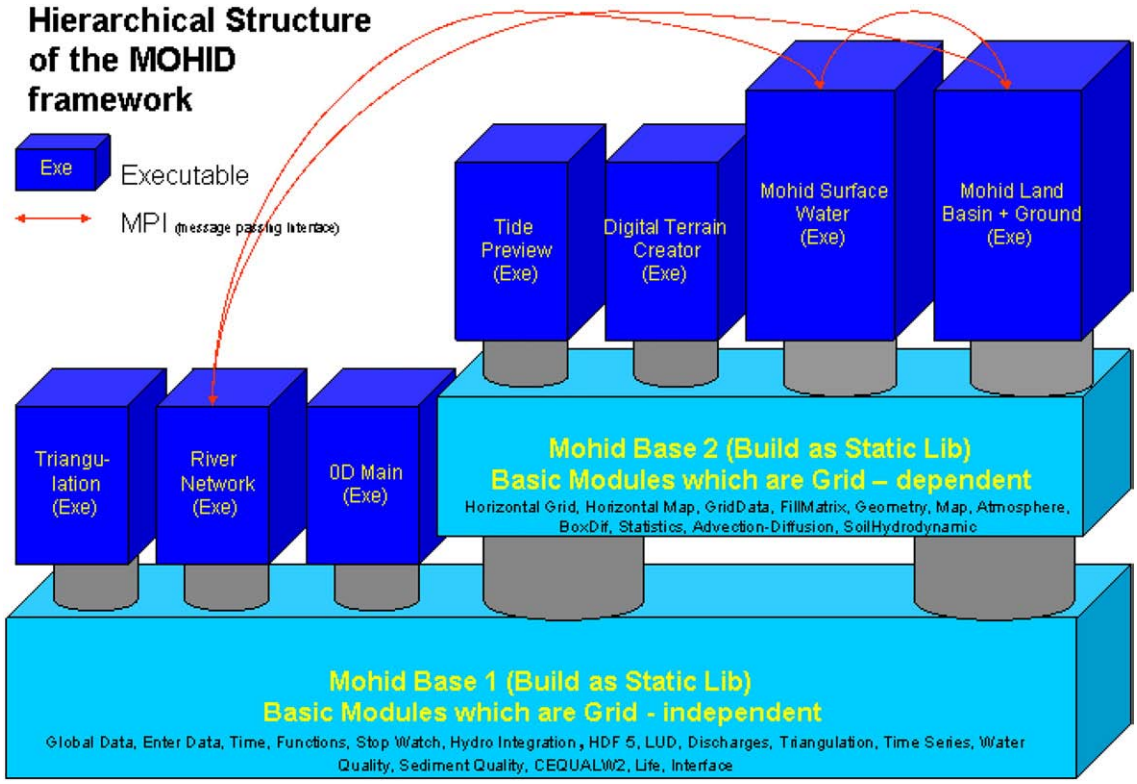

Fig. 2. Hierarchical structure of the MOHID framework.

it is easier to build conservative transport models and coupling between modules (MRN and runoff or MRN and ground water) is also simpler because it is based on fluxes.

Transport equations are derived directly from conservation principle stated in Eq. (1). In the case of momentum bottom shear is also dealt as diffusive flux.

$$\{\text{Accumulation Rate}\} = \{\text{FlowIn}-\text{FlowOut}\}_{\text{Advection}} + \{\text{FlowIn}-\text{FlowOut}\}_{\text{Diffusion}} + \{\text{Sources}-\text{Sinks}\} \quad (1)$$

Applying this conservation principle to a generic volume V contained into a surface A for a generic property with specific (per unit of volume) value β, one obtains Eq. (2).

$$\frac{\partial}{\partial t}\int\int\int_V \beta dV + \int\int_A \left(\beta \vec{v}.\vec{n}\right) dA = (\text{Diffusion}) + \{\text{Sources}-\text{Sinks}\} \quad (2)$$

In a 3D model the surface of finite volumes can have up to 6 permeable faces, while in a purely 1D model volumes have only 2 permeable faces. In the case of nodes with tributaries, an extra permeable face is considered per tributary.

For the 1D case described in this text the equations are written in the rectangular reference described in Fig. 3, where axis "x" is aligned with the river channel. In the figure are also defined the variables required for computing the driving forces.

The model can consider a generic cross section as presented in Fig. 4. In the figure P_w represents the wet perimeter (m), A_V the vertical cross sectional area (m^2) and dx the length of a volume (m). The area and the wet perimeter of the top areas of the finite volume are generally different.

When the property being transported is water, the value of β in Eq. (2) is constant and consequently its gradients are null. Treating lateral exchanges as sources/sinks of water the equation gives the continuity equation (Eq. (3)) where V is water volume (m^3) and Q_j, $j=\{\text{in, out, l}\}$ are inflow, outflow and lateral flow to the control volume ($m^3\ s^{-1}$).

$$\frac{\partial V}{\partial t} = Q_{\text{in}} - Q_{\text{out}} + Q_l \quad (3)$$

In the case of momentum, the value of β in Eq. (2) is ρv, where ρ is the water specific mass (kg m^{-3}) and v is the horizontal velocity ($m\ s^{-1}$). The sources/sinks in case of momentum are the horizontal components

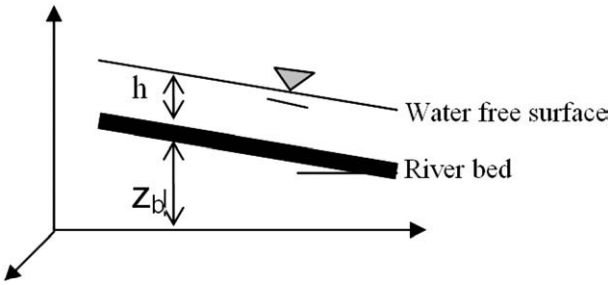

Fig. 3. Reference and main variables used: z_b is channel bottom level (m); h is water column (m); $H=z_b+h$ is the free surface level (m).

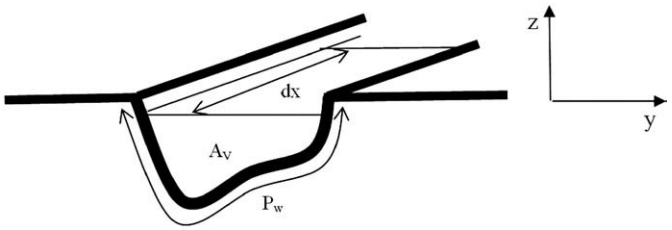

Fig. 4. Generic cross section used by the MRN.

of pressure forces in the solid and open surfaces of the control volume and shear at the bottom and at the surface. Integrating Eq. (2) in the vertical and the transversal dimensions, and neglecting surface shear because (i) it is much smaller than bottom shear and (ii) because the wind velocity is generally not aligned with the river, the St. Venant equation is obtained (Eq. (4)) where Q is water flow ($m^3\ s^{-1}$), A_V is the flow (m^2), g is gravity ($m\ s^{-2}$), h is water depth (m), $S_0 = -dz_b/dx$ is the bottom slope (–) and S_f is the bottom friction slope (–).

$$\frac{\partial Q}{\partial t} + \frac{\partial}{\partial x}(vQ) + gA_V\left(\frac{\partial h}{\partial x} - S_0 + S_f\right) = 0 \tag{4}$$

Several formulations exist in the literature to compute bottom friction slope, the most common being the Manning–Strickler resistance law, given by Eq. (5), where n is the Manning roughness coefficient ($s\ m^{-1/3}$), $R_h = A_V/P_w$ is the hydraulic radius (m) and P_w is the wet perimeter of the active cross-sectional area (m).

$$S_f = \frac{n^2}{R_h^{4/3}}\frac{Q|Q|}{A_V^2} \tag{5}$$

In steep slope channels with no backwater effects, longitudinal gradient of water depth is negligible and thus gravity forces and pressure forces balance each other. In these conditions Eq. (4) is reduced to the kinematic wave, Eq. (6).

$$S_o = S_f \Leftrightarrow Q = \frac{A_V R_h^{2/3}\sqrt{S_o}}{n} \tag{6}$$

This formulation is a simple solution but has some limitations, e.g., it's not valid when bottom slope is positive and doesn't allow for backwater effects. Applicability criteria for this and other simplifications of the St.Venant can be found in Vieira (1983). Currently, in MRN, the user has to choose the appropriate formulation.

In the case of water constituents, longitudinal diffusion associated to shear diffusion is of the same order of magnitude as advection and has to be considered. Diffusion is quantified by Fick's law of diffusion. Its contribution for Eq. (2) is given by Eq. (7), where D is diffusivity ($m^2\ s^{-1}$).

$$\text{Diffusion} = \int_A\int D\left(\vec{\nabla}\beta\cdot\vec{n}\right)dA \tag{7}$$

In a 1D case, Eq. (2) becomes Eq. (8), where F_S and F_B represent the fluxes of the property ($kg\ s^{-1}$) through the free surface (e.g. evaporation) and the bottom (e.g., infiltration, erosion and deposition), respectively.

$$\frac{\partial}{\partial t}\int_V\int\int\beta dV + \int_A\int\left(\beta\vec{v}.\vec{n}\right)dA = \int_A\int D\left(\vec{\nabla}\beta.\vec{n}\right)dA + (F_B - F_S) + (\text{Sources}-\text{Sinks}) \tag{8}$$

In the case of gases the flux across the free surface is a major term in the equation, while in the case of suspended sediments it is negligible compared with bottom flux due to erosion and/or deposition. Eq. (8) can include a settling term in case of particulate suspended matter (Section 2.5).

2.3. Computational aspects of MRN

2.3.1. Discretisation

MRN is based in a tree-like unstructured grid of nodes connected by reaches. Each node can be assigned several upstream reaches and one downstream reach, and each reach is identified by one upstream and one downstream node. Due to the finite volume approach, scalar fluxes are computed at the nodes control volumes, and vector properties (fluxes) are computed at the faces of the nodes control volumes, constituting what can be called reach control volumes (Fig. 5).

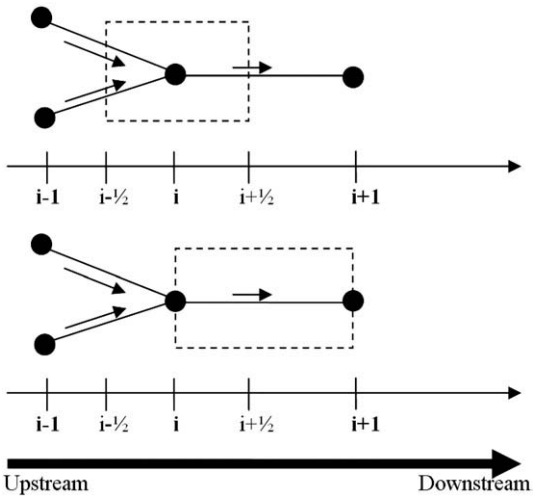

Fig. 5. Unstructured grid of MRN: Nodes (black dots) and reaches (solid line) that connect them. The dashed lines are control volumes, for nodes (top) where scalar variables are computed, and reaches (bottom) where vector variables are computed.

Cross-sectional properties are assigned for each node control volume. By default, the reach control volume cross-sectional properties are the ones given by the upstream node. Each reach has length and slope based on the extremity nodes coordinates and altitude. Each node longitudinal length is computed by the sum of half the upstream reaches length and half of the dowsntream reach length.

The continuity equation (Eq. (3)) is discretised for each node control volume as in Eq. (9), where V is volume (m^3), t is the previous computed time instant (s), $t+\Delta t$ is the current time instant (s), Q is flow ($m^3\ s^{-1}$) and j varies from 1 to the number of upstream reaches of node i.

$$\frac{V_i^{t+\Delta t} - V_i^t}{\Delta t} = \sum_j Q_{i-1/2,j}^{t+\Delta t} - Q_{i+1/2}^{t+\Delta t} \tag{9}$$

The momentum equation (Eq. (4)) is discretised for each reach control volume, being explicit on advection, pressure and gravity terms, and semi-implicit in the friction term. This approach was chosen because a full implicit algorithm in all terms would require the resolution of a sparse matrix and would be too slow. The friction term is semi-implicit for stability reasons.

The advection term is discretised with the upstream stepwise approach where it is assumed that the concentration C at left face (i-1/2) is:

$$Q_i > 0 \Rightarrow (C_{i-1/2} = C_{i-1})$$
$$Q_i < 0 \Rightarrow (C_{i-1/2} = C_i)$$

This approach states that advection can transport properties only downstream and respects the transportivity property of advection, preventing the formation of negative concentrations. The linear approach doesn't respect this property because volume "i" will get information of downstream concentration through the average process. The violation of this property can generate instabilities and will create conditions to obtain negative values of the concentration. The upstream discretisation avoids that limitation but can introduce unrealistic numerical diffusion. In MRN this is avoided by the use of "Compute Point" flags and a dynamic time step (Section 2.3.3).

Eqs. (10)–(13) present the discretisation of momentum equation, where v horizontal velocity ($m\ s^{-1}$), A_V is the cross sectional flow area of the control volume (m^2), H is the free surface level (m) and L is the longitudinal control volume length (m).

$$\frac{Q_{i+1/2}^{t+\Delta t} - Q_{i+1/2}^t}{\Delta t} = advection + pressure + friction \tag{10}$$

$$
\begin{aligned}
&advection = \frac{1}{L}\left[(uQ)_i^t - (uQ)_{i+1}^t\right]\\
&(uQ)_i = \sum_j \begin{cases} u_{i-1/2,j}Q_{ij} & , if\ Q_{ij} \geq 0 \\ u_{i+1/2}Q_{ij} & , otherwise \end{cases}\\
&Q_{ij} = \frac{Q_{i-1/2,j} + Q_{i+1/2}}{2}\\
&(uQ)_{i+1} = \begin{cases} u_{i+1/2}Q_{i+1} & , if\ Q_{i+1} \geq 0 \\ u_{i+3/2}Q_{i+1} & , otherwise \end{cases}\\
&Q_{i+1} = \frac{Q_{i+1/2} + Q_{i+3/2}}{2}
\end{aligned}
\tag{11}
$$

$$
pressure = gA_{V,i}^t\left(\frac{H_i^t - H_{i+1}^t}{L_{i+1/2}}\right) \tag{12}
$$

$$
friction = -gA_V S_f = -g[n^2 Q^t Q^{t+\Delta t}]_{i+1/2}/[(R_h^t)^{4/3}A_V^t]_i \tag{13}
$$

If the kinematic wave approach is used, the momentum discretisation is simply Eq. (14).

$$
Q_{i+1/2}^{t+\Delta t} = \frac{A_{V,i}^t (R_{h,i}^t)^{2/3}}{n_{i+1/2}}\sqrt{\frac{z_i - z_{i+1}}{L}} \tag{14}
$$

The scalar properties transport equation is discretised in node control volumes, and is explicit in time, using upstream stepwise approach for advection and central differences for diffusion.

$$
\frac{(\beta V)_i^{t+\Delta t} - (\beta V)_i^t}{\Delta t} = \text{advection} + \text{diffusion} + (F_B - F_S) + (\text{sources} - \text{sinks}) \tag{15}
$$

$$
\begin{aligned}
&advection = (\beta^t Q^{t+\Delta t})_{i-1/2} - (\beta^t Q^{t+\Delta t})_{i+1/2}\\
&(\beta Q)_{i-1/2} = \sum_j \begin{cases} \beta_{i-1,j}Q_{i-1/2,j} & , if\ Q_{i-1/2,j} \geq 0 \\ \beta_i Q_{i-1/2,j} & , otherwise \end{cases}\\
&(\beta Q)_{i+1/2} = \begin{cases} \beta_i Q_{i+1/2} & , if\ Q_{i+1/2} \geq 0 \\ \beta_{i-1} Q_{i+1/2} & , otherwise \end{cases}
\end{aligned}
\tag{16}
$$

$$
\begin{aligned}
&diffusion = D\left[\left(\frac{\partial\beta}{\partial x}A_V\right)_{i-1/2} - \left(\frac{\partial\beta}{\partial x}A_V\right)_{i+1/2}\right]\\
&\left(\frac{\partial\beta}{\partial x}A_V\right)_{i-1/2} = \sum_j\left(\frac{\beta_i - \beta_{i-1,j}}{L_{1-1/2,j}}\right)\left(\frac{A_{V,i} + A_{V,i-1,j}}{2}\right)\\
&\left(\frac{\partial\beta}{\partial x}A_V\right)_{i+1/2} = \left(\frac{\beta_{i+1} - \beta_i}{L_{1+1/2,j}}\right)\left(\frac{A_{V,i+1} + A_{V,i}}{2}\right)
\end{aligned}
\tag{17}
$$

In order to guarantee mass conservation for scalar properties the discretisation of the advection diffusion equation and of continuity equation must be consistent. When lateral affluences exist, they must also be accounted in the continuity equation and in the advection–diffusion equation on the same time instants.

Currently, MRN can compute cross sectional flow area, water depth, wet perimeter and hydraulic radius from volume for rectangular, trapezoidal, given height, bottom and top width, and irregular cross sections, given station and elevation coordinates.

2.3.2. Downstream boundary condition

Without user restrictions, the outlet reach flow is computed with the kinematic wave because its downstream node is not a compute point of the model (it only defines outlet location and slope). However, user can impose a constant flow at the outlet (e.g. no flow) or time variable water depth at the outlet (e.g. tide).

2.3.3. Dynamic time step

MRN uses a dynamical time step in its main hydrodynamic cycle. Within an iterative cycle, if the water volume of any reach varies more than a user defined percentage during two consecutive time steps, the model automatically decreases the time step and recalculates the current solution with a smaller time step. This process is repeated until the volume variation is less than the user defined value mentioned above. The time step dynamically increases again when the model verifies that flow is "stable". Simulations made with MRN have shown that time step may be reduced to very short intervals during flush events.

This procedure avoids negative volumes and optimizes simulation time cost, without compromising model stability. This is particularly important in explicit methods and to avoid numerical dispersion. Time steps of the processes computed in different sub-models, such as water quality, can be defined differently, adding more to the optimization of simulations computational cost.

2.4. Biogeochemical modules

MOHID can simulate the cycles of carbon, nitrogen, phosphorous and oxygen occurring both in the water column and in the benthos. Interactions between water constituents (e.g. nutrients, algae, sediments, pollutants) are modelled through the sources and sinks terms in Eq. (2). The processes are 0D and were implemented in separate modules, making them grid-independent and thus accessible to all MOHID executables. (ocean, estuary, basin, river). The time step used for these 0D models is also independent from the hydrodynamic time step thus improving computational costs.

The pelagic processes are programmed in a module called water quality and were adapted from well-known ecological models such as WASP (Wool et al., 2001) and CE-QUAL-W2 (Cole and Wells, 2003), and further enhanced with bacterial decay and macroalgae (Trancoso et al., 2005). The water quality module can be used with Eulerian or Lagrangian transport modules, and considers 18 properties, including nutrients and organic matter (nitrogen, phosphorus and silica biogeochemical cycles), oxygen and organisms (phytoplankton, zooplankton and heterotrophic bacteria in the water column).

Recently, a new, more robust, pelagic ecological model was added to MOHID, ModuleLife, which is based on ERSEM model (Baretta et al., 1995) and, unlike the other models, has a decoupled carbon-nutrients dynamics with explicit parameterization of C, N, P, Si, and O cycles. It considers two major groups of producers in the system, diatoms and autotrophic flagellates. All living and organic matter compartments of the model have variable stoichiometry (Mateus, 2006).

The benthos module was developed to compute biogeochemical processes occurring in the benthic compartment, namely at the water-sediment interface (Fernandes et al., 2006). In this module, as in other MOHID modules, variables can be considered to have particulate or dissolved phases. Particulate phases can settle and deposit at the bottom of the water column, and while they are deposited there are further biogeochemical processes being computed that will determine their fate. Thus, several processes are computed, including: (i) Algae mortality, if algae are considered as a particulate property that can sink and deposit, then if deposited a mortality rate is applied; (ii) particulate organic matter mineralization (nitrogen and phosphorus biogeochemical cycles); (iii) biogenic silica dissolution; (iv) oxygen depletion; (v) growth of heterotrophic bacteria in the river bed (often caused by point source inputs in dry phases where shear stresses are low).

The benthos module is also readily coupled, in terms of organic matter mineralization, biogenic silica dissolution and oxygen depletion, with other pelagic biogeochemical models included in MOHID as described above.

2.5. Sediments transport model

MOHID is able to partition transported properties between dissolved and particulate phases through adsorption–desorption mechanisms with suspended cohesive sediments. These are subject to deposition and erosion processes, which are also simulated by MOHID, determining the equilibrium between dissolved and particulate matter (Cancino and Neves, 1999a,b). This is a very important feature in pollutants fate modelling, particularly in rivers where, for instance, flush events release

high amounts of sediments and their adsorbed pollutants. The sediments transport model is fully described in Cancino and Neves (1999a) but here resumed.

The erosion and deposition algorithms are based on the assumption that these processes never occur simultaneously. Erosion occurs when the ambient shear stress exceeds the threshold of erosion. The flux of eroded matter is given by Eq. (18), where E is the erosion constant (kg m^{-2} s^{-1}), τ is the bed shear stress (Pa), τ_E is a critical shear stress for erosion (Pa) and C and C_S are the deposited concentrations of the particulate property and sediments at the water bed interface, respectively (kg m^{-2}).

As with erosion, deposition occurs when the ambient shear stress is lower than a specified threshold. The flux of deposited matter is given by Eq. (19), where τ_D is a critical shear stress for deposition (Pa), C is the suspended particulate property (kg m^{-3}) and w_s is the settling velocity (m s^{-1}), which can be calculated with several formulations.

$$\frac{\partial M_E}{\partial t} = \begin{cases} E\left[\frac{C}{C_S}\right]_B \left(\frac{\tau}{\tau_E} - 1\right) & , if\ \tau > \tau_E \\ 0 & , otherwise \end{cases} \quad (18)$$

$$\frac{\partial M_D}{\partial t} = \begin{cases} C w_s \left(1 - \frac{\tau}{\tau_D}\right) & , if\ \tau < \tau_E \\ 0 & , otherwise \end{cases} \quad (19)$$

2.6. Coupling of MRN with run-off models

When running as a standalone model, MRN needs to import results from the basin as point discharges in the river heads. For this reason, MRN can been coupled to SWAT model, through an interface developed at MARETEC (Chambel-Leitão et al., 2007). MRN imports surface runoff, lateral flow, groundwater flow and concentrations of water constituents from SWAT as input discharges. Property concentrations can be considered constant (user supplied) or can be an output of SWAT model.

Nevertheless, MRN can be coupled with any model if their inflows are transformed into the MOHID discharge files. These are simple ASCII files with flows and concentration of properties (nutrients, temperature, etc). For example, Obermann (2007) used results coming from Mercedes model as inflow for MRN.

2.7. Transmission losses, evaporation and pools

Transmission losses and pools are important features in semi-arid regions. Transmission losses are due to permeable river beds and soils (infiltration) and high temperatures in summer (evaporation). When coupled to MOHID Land, river channels can loose or gain water, depending on the hydraulic gradient between the water level in the channel bed (or pools) and the level of the aquifer. This approach is possible because MOHID Land explicitly simulates the level of the aquifer (Galvão et al., 2004). When running MRN as standalone, water from the channels (or from the pools) can infiltrate the river bed at a constant user defined rate, defined as the saturated conductivity of the sediments in the channel bed. This is an approximation, since conductivity depends on water content and the infiltration capacity of

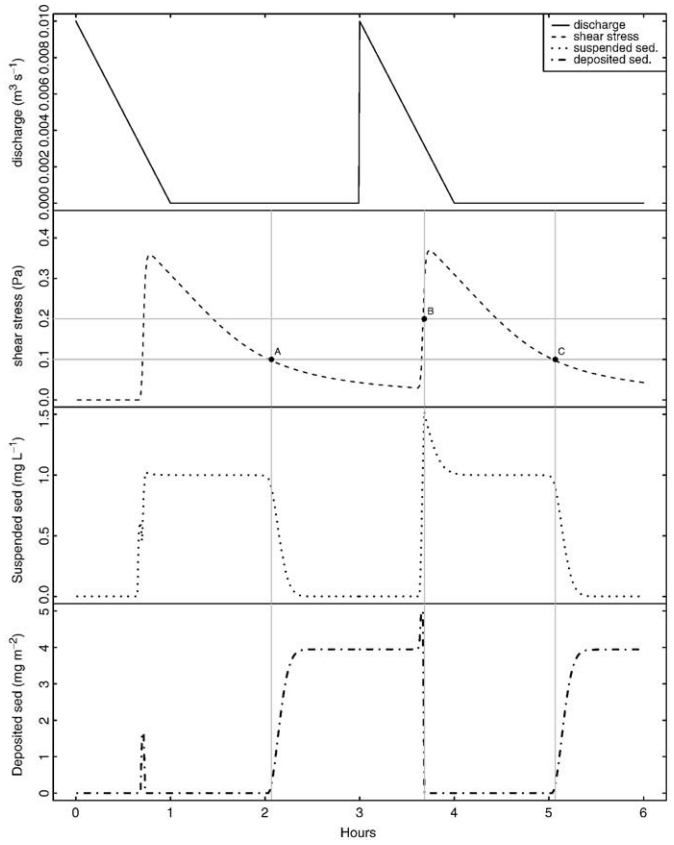

Fig. 7. From top to bottom: time series of discharge, shear stress, suspended and deposited sediments at the 50th reach. Deposition (A, C) and erosion (B).

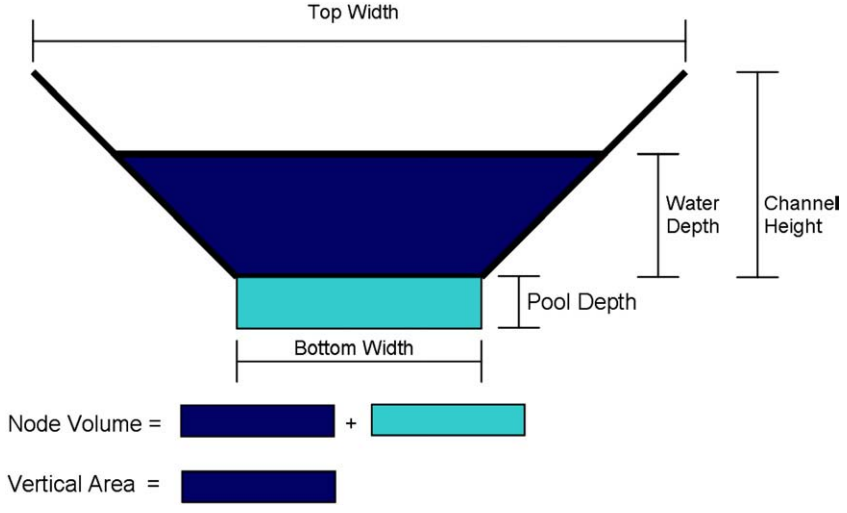

Fig. 6. Pool modelling in MRN.

the sediment. Transmission losses are also important in the accumulation of particulate matter in the channel bed. Evaporation will increase the concentration of all properties (dissolved or particulate) in the water column, since the model considers that only "pure" water evaporates. MRN computes sensible and latent heat fluxes from water to atmosphere given the necessary atmospheric conditions (solar radiation, air temperature, wind speed and relative humidity).

Pools accumulate sediments and concentrate pollutants that are released in the first flood event of the hydrological year. They can be modelled as storage volumes in specified nodes of the tributary network, characterized by a pool depth (Fig. 6). The total node volume increases to account for the pool, but the active flow vertical area of the cross-section (A_V) is not affected by the pool, because flow from that node only starts when the pool is full and water starts to fill the "active volume" of the node.

3. Verification examples

In a real river system, all the processes occur and interact to produce the complex hydrodynamics, sediments and water quality dynamics. Therefore, in a new model, it is important to verify in schematic cases if the processes are being well simulated prior to including them in a real case study. In schematic tests we can control which processes are occurring and what is to be expected. This section begins with tests on the most important processes for semi-arid streams, both at the hydrodynamic level (pools and transmission losses), sediments transport and water quality (specifically coliform decay). Next, a real case study is presented in Trancão basin where hydrodynamics in the streams is verified against gauge stations. In this case, MRN is used within MOHID Land to compute the correct boundary conditions to the stream network.

The verification examples aim to show MRN's ability to model stream events. Other features pertaining to modules already validated (e.g. ecological models) are not included in this paper.

3.1. Processes verification on schematic river

The processes verification tests are based in a schematic river of length 1 km (comprised of 100 reaches with 10 m length each) and slope 0.001, and no tributaries. Cross sections were chosen to be rectangular with 1 m bottom width. Manning roughness coefficient was chosen to be 0.02, which, according to Chow (1959) corresponds to channels with earth material, smooth irregularities, without cross section variations, and without obstructions, vegetation or meandering.

3.1.1. Erosion and deposition of sediments

This test case verifies the erosion and deposition processes of sediments, which is a determinant aspect of ephemeral waters quality. Sediments were discharged with 1 mg L^{-1} concentration into the dry schematic river. The discharge flow is not constant as presented in the top panel of Fig. 7. The other panels show (from top to bottom) the shear stress, suspended and deposited sediments concentration. Critical erosion and deposition shear stresses were 0.1 and 0.2 Pa respectively, which are the commonly used values for cohesive sediments. Settling velocity was considered constant and equal to 10^{-4} m s^{-1}. The figure shows that at the arrival of the first flood event deposition occurs in a small time window when shear stress is still below 0.1 and there are already some suspended

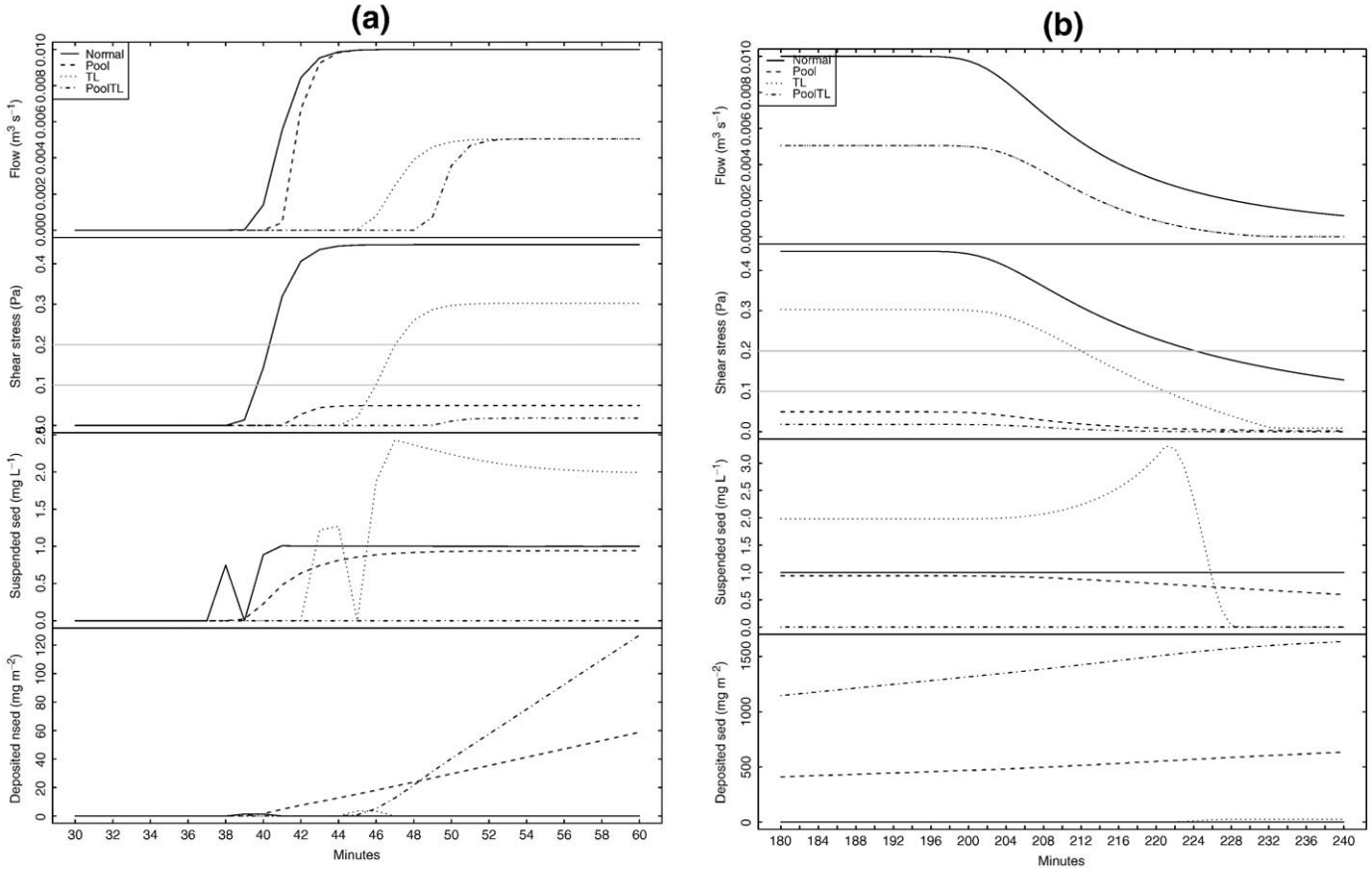

Fig. 8. From top to bottom: Time series of flow, shear stress, suspended and deposited sediments concentration, at the 50th reach when a 3 h discharge of 0.01 m^3 s^{-1} discharge with 1 mg L^{-1} of suspended sediments is made the dry schematic river, in the following conditions: Normal—no transmission losses or pools are simulated; Pool—with is a 0.1 m depth pool in the 50th reach of the river; TL—without pools but with transmission losses along the river. Left panel (a) shows the arrival, and right panel (b) shows the decay of the flood wave.

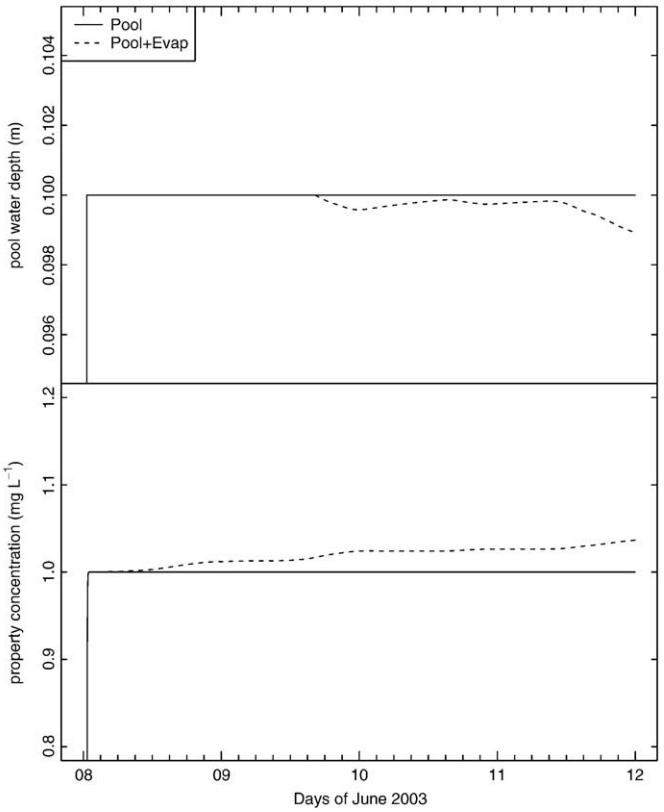

Fig. 9. Time series evolution of the pool water depth (top panel) and a generic property concentration, without evaporation ("Pool" run) and with evaporation fluxes ("Pool+Evap" run).

sediments. However, these are immediately eroded when the shear stress increases above 0.2. After the first flood event when the shear stress drops below 0.1 Pa (point A) deposition of suspended sediments occurs. When the second flood arrives and shear stress rises above 0.2 (point B) the deposited sediments are eroded and suspended sediments concentration increases. The spike in the suspended sediments concentration occurs in the small time window when there is no deposition or erosion (shear stress between 0.1 and 0.2). Again, after the flood, deposition starts at point C. These results verify that erosion and deposition processes are correctly simulated.

3.1.2. Pools and transmission losses

This test verifies the effects of pools and transmission losses on the hydrodynamics and sediment dynamics. A discharge of 0.01 m^3 s^{-1} with 1 mg L^{-1} of suspended sediments during 3 hours was imposed upstream the schematic river, without pools or transmission losses, ("Normal" run), with a 0.1 m depth pool at the middle of the river (50th reach) initially half filled with "clean" water ("Pool" run), without pools but with a transmission loss hydraulic conductivity of 0.01 mm s^{-1} ("TL" run), and with the pool and transmission losses ("Pool TL" run). The river is initially dry and there are no deposited sediments. Erosion and deposition parameters for the sediments are the same as in Section 3.1.1.

Before discussing the implications of pools and TL, it is important to note that, as evidenced by the "Normal" run, flow and sediments concentration gradually reach the discharged values (Fig. 8a,b), indicating that the model conserves mass and momentum.

At the arrival of the flood (Fig. 8a) and in the "Normal" run, sediment deposition occurs only in a small time window while shear stress is below 0.1 Pa. This small amount of sediment is immediately eroded as shear stress rives above 0.2 Pa. There is no further erosion because there are no deposited sediments. With the pool, the flood wave arrives later due to the time taken to fill the pool with water. Sediments concentration is diluted by the clean water in the pool and the steady state concentration is attained at a later period. The steady state concentration is below unity due to deposition occurring in the pool, as indicated by the shear stress being always below 0.1 Pa, and the increasing deposited sediments concentration. With TL, the flood wave arrives even later and with lower magnitude, due to infiltration. After the rise of the flood wave, suspended sediments concentration is higher than discharged (>1 mg L^{-1}) because the infiltration process only transfers water and dissolved properties, acting as a filter on particulates, which accumulate in the channels. The simulation of the pool and TL shows the combined effect of the two previous simulations, with the pool being determinant for sediment deposition to occur, and TL for the increase in deposited sediments concentration.

After 3 hours, when the discharge stops (Fig. 8b) and the shear stress drops below 0.1 Pa, deposition starts to occur in the "Normal" run (only after the 4th hour, not shown here) and in the "TL" run. In the "Pool" and "Pool TL" run, deposition fluxes increase because shear stress decreases further. As expected, in the "TL" run, suspended sediments concentration increases while the shear stress is above 0.1 Pa but flow is decreasing. This surge in suspended sediments concentration is a critical issue in stream water quality studies after precipitation events.

3.1.3. Pools and evaporation

The effect of evaporation in ephemeral waters can be better analysed in an isolated pool subject to atmospheric heating. To verify this, take the simulation conditions described in the previous section for the "Pool" run, and add to the discharge a generic property 1 mg L^{-1} concentration and 15 °C of temperature. Solar radiation, relative humidity, wind speed and air temperature were taken from the meteorological station used in the real case study (Section 3.2). In about 4 hours, the discharge leaves the river empty and the pool filled with this generic property. Fig. 9

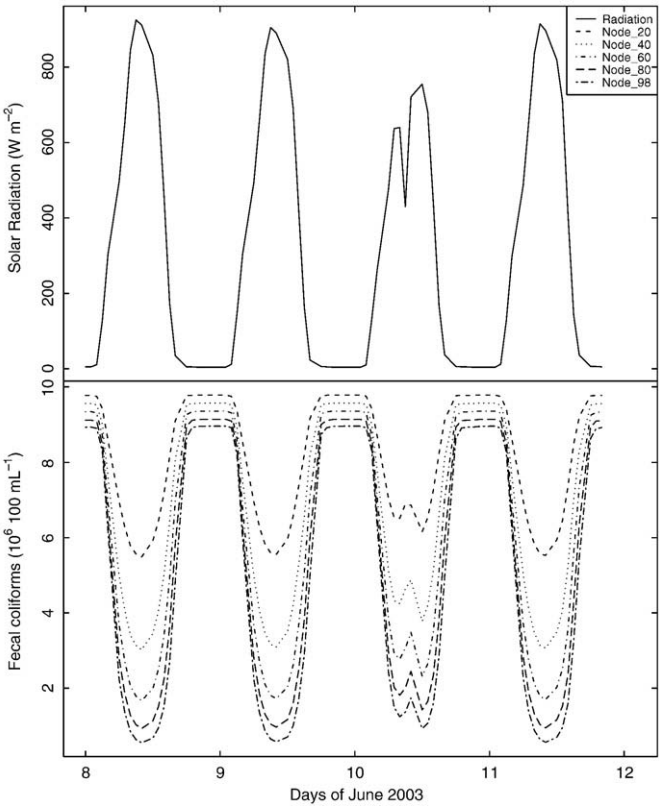

Fig. 10. Time series of solar radiation (top) and coliform concentration in several nodes (Node IDs increase downstream).

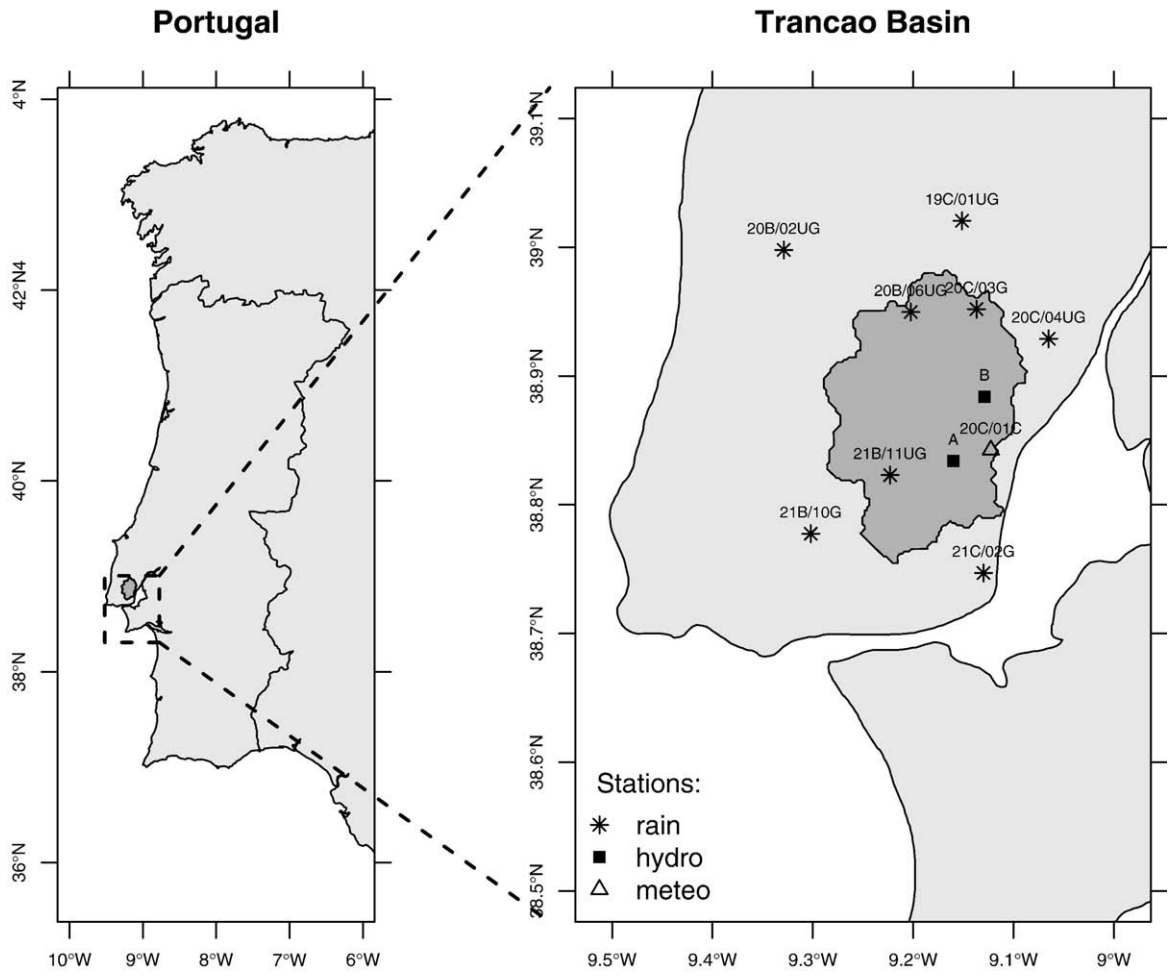

Fig. 11. Geographical location of Trancão basin (dark grey enclosed area in the right panel) and location of rain, hydrometric and meteorological stations.

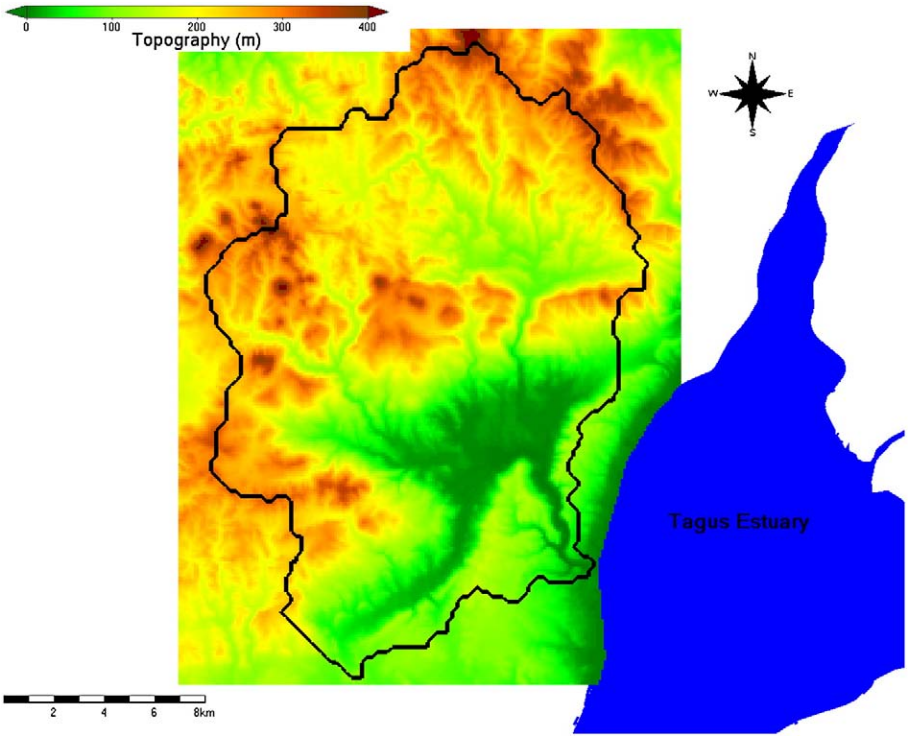

Fig. 12. River network over topography of Trancão basin. The blue polygon at the right is a representation of Tagus Estuary, where Trancão discharges. (For interpretation of the references to colour in this figure legend, the reader is referred to the web version of this article.)

Table 1
Parameters associated with land use categories, from Corine Land Cover data set (2000)

Parameter	Urban	Crop	Forest	Reference
Impermeable area (%)	50	0	0	estimated
Leaf area index (m^2 m^{-2})	1.2	1–4	5.0	(Valente et al., 1997; van Dijk and Bruijnzeel, 2001).
Specific leaf storage (mm)	0,6	0,1–0,6	0,1	(Valente et al., 1997; van Dijk and Bruijnzeel, 2001).
Manning–Strickler's roughness coefficient (s $m^{-1/3}$)	0,01	0,4	0,8	(Panday and Huyakorn, 2004; Beeson et al., 2001).
Evapotranspiration coefficient (–)	1,0	0,3–1,15	1,0	Feddes et al. (2001).
Feddes parameter "h1" (m)	−0,1	0,0	−0,1	Feddes et al. (2001).
Feddes parameter "h2" (m)	−0,25	−0,01	−0,25	Feddes et al. (2001).
Feddes parameter "h3" (m)	−5,0	−7,0	−6,0	Feddes et al. (2001).
Feddes parameter "h4" (m)	−30,0	−30,0	−30,0	Feddes et al. (2001).
Root depth (m)	0,5	0,2–0,4	1,0	Feddes et al. (2001).

Table 2
Hydraulic properties of soil types considered in the case study

Parameter	Coarse/Medium	Medium/Fine	Fine/Very fine
Porosity (m^3 m^{-3})	0.3859	0.4323	0.4903
Maximum hydraulic conductivity (cm day^{-1})	30.7	6.1	16.9
"Alpha" parameter	2.75	1.37	2.14
"n" parameter	1.390	1.391	1.193

compares results in the pool with and without evaporation. As expected, water evaporates from the pool, decreasing its depth (top panel) and increasing the concentration of the property (bottom panel).

3.1.4. Coliform decay

The concentration of coliform bacteria in water is one of the most important parameters to determine its quality. To verify if MRN correctly simulates coliform decay with atmospheric interaction, a constant discharge of 0.01 m^3 s^{-1} with 10^7 100 mL^{-1} coliforms, 10 °C and zero salinity was imposed at the upstream part of the dry schematic river. Coliforms decay followed Cantera's decay formulation (Canteras et al., 1995). Solar radiation was taken from the meteorological station used in the real case study (Section 3.2) as shown in Fig. 10 top panel. The bottom panel of Fig. 10 shows the temporal evolution of coliform concentration at a series of nodes progressing downstream. As expected, coliform concentration decreases at mid-day, with less intensity in the third day, which corresponds to a cloudy day, as indicated by the lower peak radiation. The troughs of low concentration intensify and widen as the flow progresses downstream, indicating the correct simulation of coliform decay.

3.2. Hydrodynamic validation in real case study

MRN hydrodynamics was validated in Trancão basin (Fig. 11), which is a small heavily industrialized and densely populated catchment in the northern part of Lisbon that discharges into the Tagus Estuary, one of the largest in Europe. Although with an overall reasonable water quality (Saraiva et al., 2007), Tagus estuary has still some pollution "spots" which is the case of the mouth of Trancão River. This basin was chosen as a case study due to its environmental importance and to the existence of long series of both hydrological and meteorological data. MRN was used coupled to MOHID Land, with runoff, precipitation, evaporation and infiltration processes, in a 4 years simulation (from October 1st 2002 to September 30th 2006).

In this section we present the simulation conditions and hydrodynamics validation with water depth measurements at stations A and B (Fig. 11).

The digital elevation model (DEM) used to delineate Trancão Basin had 200 m of resolution and was obtained from the Shuttle Radar Topography Mission (SRTM) DEM data (Hounam and Werner, 1999). Elevations range from 0 to 421 m above sea level. The total drainage area is 293 km^2. The river network was created with MOHID GIS (Braunschweig et al., 2005), by assigning an outlet point and an upstream minimum drainage area, to the drainage directions in the DEM. Drainage direction in each cell is towards the steepest slope of

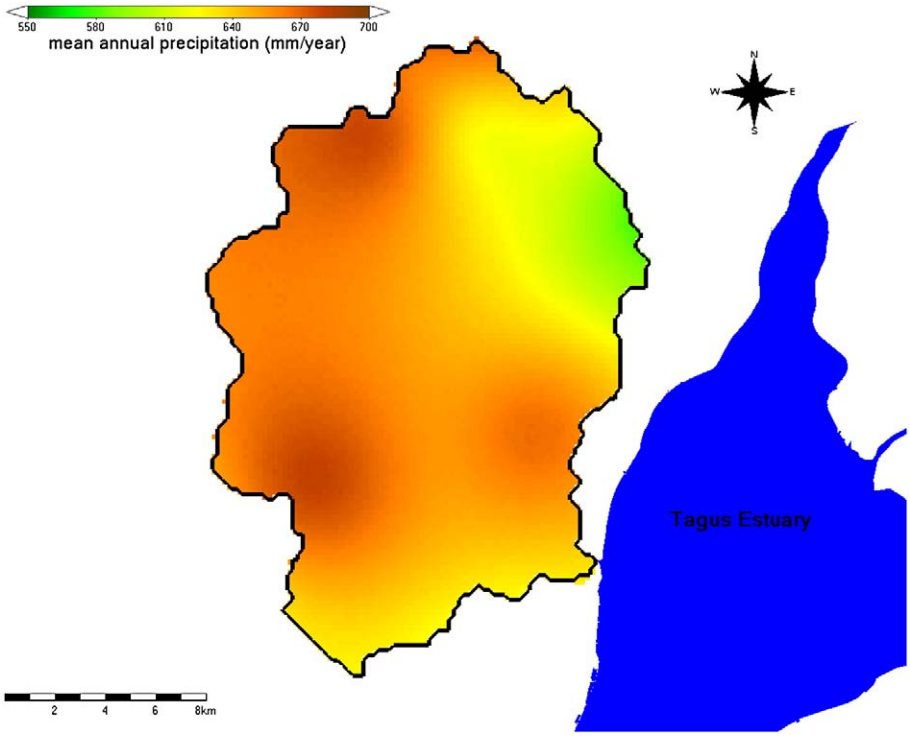

Fig. 13. Mean annual precipitation, between 2002 and 2005, in Trancão basin.

the 8 surrounding cells. Before this, the software removes DEM depressions by assigning new values to the depression pixels having the lowest value found along the depression boundary (Emaruchi, 1998).

The river network obtained with a threshold drainage area of 10 ha is presented in Fig. 12 over the DEM, being well correlated with the 1:25,000 Military Maps (Portuguese Army Geographical Institute). Some mismatches occur in plain areas and where there was human intervention. In streams enclosed by dikes created for irrigation strategy, the DEM was corrected to produce the correct stream lines.

Proper land use discrimination in a basin model is important because it determines (i) rain retention by leaves and (ii) flow resistance, which influences runoff flow, and (iii) permeability of soil which influences infiltration flow. Land use was obtained from Corine Land Cover data set released in 2000 (http://dataservice.eea.europa.eu/dataservICE) and three categories were used (urban, crop and forest, taken from the level 1 classes). Table 1 show parameter values associated with the land use categories. The impermeable area is the percentage of each grid cell unavailable for infiltration. In pavement areas this value could reach 100% but due to the presence of parks and other green areas, this value was considered not to be above 50%. Leaf Area Index is a parameter that quantifies the area occupied by leafs by horizontal square meter. Together with the Specific Leaf Storage parameter they indicate the amount of rain intercepted by leaves before reaching the ground.

Soil hydraulic parameters are necessary to compute infiltration and flow in the saturated and unsaturated zones. The 3 dimensional soil model of MOHID Land needs these parameters both horizontally and vertically discretised. As with many other basins there are no such measured data for Trancão basin, but they can be estimated from soil type maps and pedotransfer functions. The soil types were obtained from the European Environment Agency data center (1:1,000,000) (Vossen and Meyer-Roux, 1995). The pedotransfer functions (PTFs) were based on texture producing van Genuchten hydraulic properties for retention and conductivity in the soil (van Genuchten, 1980; Schaap and Leij, 1998). Schaap and Leij (1998) developed neural network PTFs to predict soil water retention, saturated and unsaturated hydraulic properties from limited or more extended sets of soil properties. In the present case only texture was available, which means that the most basic PTF was used. The PTFs developed by Schaap and Leij (1998) are included in a Windows 95/98 program called ROSETTA, which was used to obtain the soil parameters. These soil properties (Table 2) were admitted constant in depth, accounting however for soil thickness, which was considered to be linearly proportional to surface slope. Soil had a minimum depth of 2.5 m where slope was higher than 28% and a maximum depth of 30 m for slopes of zero. Soil porosity indicates the fraction of empty spaces per unit of soil volume. These spaces are filled with water when the soil is saturated, and then freed from water in the drying process. Hydraulic conductivity measures the easiness of water to flow in a porous medium, thus increasing with porosity. It has a maximum when the soil is saturated. The "alpha" and "*n*" parameters are used in the van Genuchten approximation (van Genuchten, 1980) to the pF curve, which relates suction power with water content.

Meteorological forcing is given by precipitation, solar radiation, air temperature, wind speed, relative humidity and cloud cover. The last four parameters will determine evapotranspiration fluxes magnitude. Due its high spatial variability, precipitation data was horizontally interpolated with the inverse weighted distance method for the 8 rain gauges and the meteorological station (20C/01C) nearby Trancão basin (Fig. 11). All other meteorological parameters were taken from the meteorological station and considered constant in space. All this data are publicly available from the Portuguese National Water Institute (www.snirh.pt). Fig. 13 shows the spatial gradients of the mean annual precipitation (between 2002 and 2005) and thus the importance of having spatial variable precipitation in Mediterranean basins such as this.

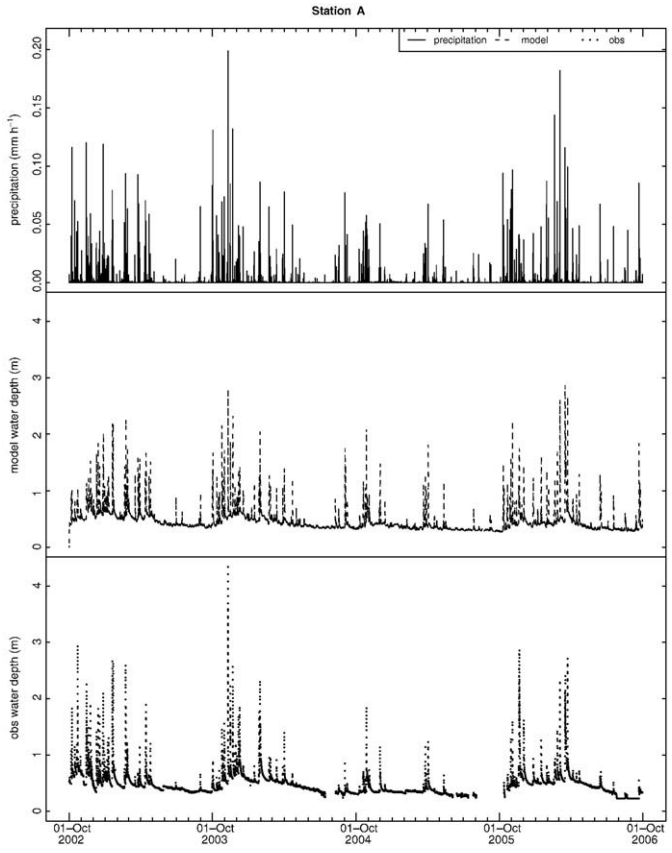

Fig. 14. From top to bottom: time series of precipitation, simulated and observed water depth at station A.

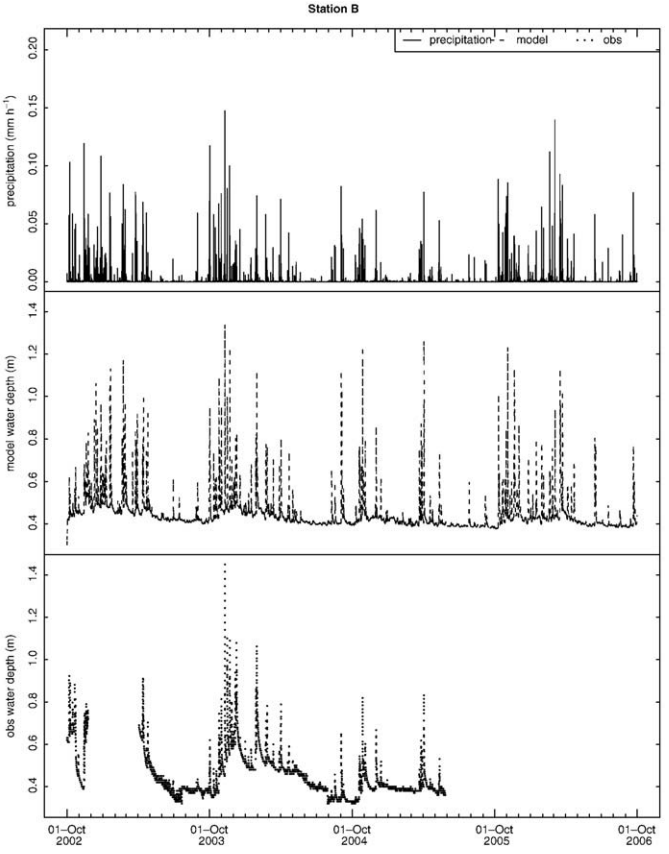

Fig. 15. From top to bottom: time series of precipitation, simulated and observed water depth at station B.

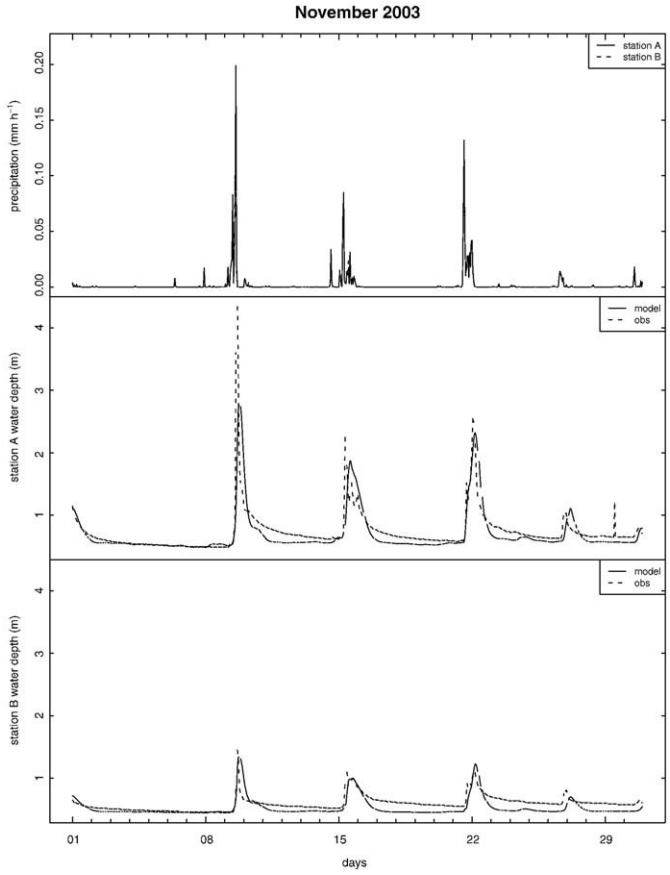

Fig. 16. Time series of precipitation at station A and B (top panel), station A modelled and observed water depth (middle panel) and station B modelled and observed water depth error (bottom panel) for November 2003.

The simulation (4 years, 300×300 grid cells, 13 soil layers and 2748 nodes in the drainage network) was complete in approximately 7.5 hours in a 2.4 GHz processor with 2 GB RAM.

Figs. 14–16 and Table 3 show the comparison of model results with measured data. In Table 3, observations and model results are referred with subscript *obs* and *mod* respectively, values in parenthesis are relative to the observed mean, x is mean value, σ is standard deviation, bias $= x_{\mathrm{mod}} - x_{\mathrm{obs}}$ is the mean error, rmse $= \sqrt{\sum (x_{\mathrm{mod}} - x_{\mathrm{obs}})^2 / N}$ is the root mean square error, N is the total number of data points, R^2 is the correlation coefficient, and $\eta = 1 - \sum (x_{\mathrm{mod}} - x_{\mathrm{obs}})^2 / \sum (x_{\mathrm{obs}} - \bar{x}_{\mathrm{obs}})^2$ is the Nash–Sutcliffe coefficient (or model improvement over climatology).

For station A, Fig. 14 shows that the model simulates the timing of water level peak events and their relative intensity. This was expected due to the relatively small size of the basin and discrete rainfall events. Flow decay after precipitation events is also properly simulated. This is corroborated by the high correlation coefficients and low relative bias and rmse (Table 3). The model overestimates water depth in less than 31% of the mean observed value for this location, having an efficiency of approximately 50%, revealing an adequate spatial interpolation for precipitation and runoff parameterization. Because water losses take place mainly trough infiltration, the above sustains that soil parameterizations are adequate and the infiltration process is well simulated.

For station B, Fig. 15 shows that the timing of the water level peaks is in accordance with observations but their intensity is overestimated. Also, base flow retained in this site after the several rainfall events is not simulated. These last two aspects can be due to the complex river cross section nearby this station. The station is located in a valley where the river bed is highly irregular and filled with large rocks. Water retained in these irregularities can be released when there is no precipitation. This is supported by the lower correlation coefficients and lower model efficiency (34%) compared to station A. rmse has lower relative values in this station because standard deviations and bias are also lower.

To verify model's performance on shorter time scales, three precipitation events that occurred in November 2003 were analysed separately. The top panel in Fig. 16 shows precipitation at the two stations, with peaks occurring at the same time, but with lower intensity in station B. From the middle and bottom panels, the correct simulation of timing of the water level peaks can be clearly verified, as well as the approximate simulation of flow decay after each precipitation event. The model slightly underestimates water level in these occasions, which can be due to unaccounted irregularities at the station's cross section. The differences in precipitation in the two stations and the good level results enfatize the importance of the spatial variability of precipitation in semi-arid basins, even as small as this one.

In summary, for station A, the model can simulate the real rating curve and that there is an adequate relationship between precipitation/infiltration/flow processes. For station B, the rating curve is not well simulated by MRN most probably due to the complexity of the cross sections nearby this station. However, this is not a strong conclusion for station B because there is no measured data for two of the three main flood events.

4. Conclusions

This paper describes MRN model as 1D hydrodynamic model for river networks whose development was especially focused on the reproduction of processes occurring in temporary river networks (flush events, pools formation, infiltration and evaporation). Unlike many other models, it allows the quantification of settled materials at the channel bed also over periods when the river falls dry. These features are very important to secure mass conservation in highly varying flows of temporary rivers. MRN accommodates several numerical hydrodynamic momentum approximations (from the simple kinematic wave to the full St. Venant equation), being discretised on finite volumes, guaranteeing mass and momentum conservation. It has a dynamic time step that adapts to the actual flow conditions, guaranteeing numerical stability. The river network can be easily constructed from a DEM using MOHID GIS, where cross sectional properties, such as geometry and friction parameters, can be assigned to nodes.

Table 3
Statistical analysis of the observed and simulated water depth in stations A and B stations

		Hourly	Daily	Monthly	Nov 2003
Station A	x_{obs}(m)	0.480	0.476	0.465	0.749
	x_{mod}(m)	0.491	0.487	0.480	0.702
	σ_{obs} (m)	0.208	0.183	0.141	0.358
	σ_{mod} (m)	0.227	0.195	0.128	0.357
	Bias (m)	0.010 (2%)	0.010 (2%)	0.015 (3%)	−0.047 (−6%)
	rmse (m)	0.149 (31%)	0.111 (23%)	0.070 (15%)	0.230 (31%)
	R^2 (−)	0.773	0.830	0.873	0.801
	η(%)	49%	69%	75%	59%
Station B	$\bar{x}_{obs}$ (m)	0.448	0.447	0.448	0.599
	$\bar{x}_{mod}$ (m)	0.449	0.448	0.450	0.530
	σ_{obs} (m)	0.102	0.098	0.085	0.123
	σ_{mod} (m)	0.080	0.068	0.039	0.148
	Bias (m)	0.002 (0.4%)	0.001 (0.2%)	0.001 (0.2%)	−0.069 (−12%)
	rmse (m)	0.083 (18%)	0.076 (17%)	0.061 (14%)	0.114 (19%)
	R^2 (−)	0.608	0.635	0.739	0.795
	η (%)	34%	40%	47%	15%

Observations and model results are referred with subscript *obs* and *mod* respectively. Values in parenthesis are relative to the observed mean.

MRN is part of MOHID Water Modelling System, which is a modular system for the simulation of water bodies (hydrodynamics and water constituents). As such, MRN is capable of simulating water quality in the aquatic and benthic phase and have a 2-way interaction with MOHID Land, which computes runoff and porous media transport, allowing for the dynamic exchange of water and materials between the river and surroundings. These features account for spatial gradients in precipitation which can be significant in Mediterranean-like basins. Nevertheless, MRN can receive discharges at any specified nodes thus allowing it to be used as a standalone model, resolving transport given by other basin models. An interface has been already developed for SWAT basin model.

MRN's specific processes for ephemeral waters were verified in schematic tests and hydrodynamics was validated in a 4 years simulation in Trancão basin, coupled to MOHID Land. Results were promising, with Nash–Sutcliffe coefficient above 34% in hourly time series of water depth, indicating that the model is able to correctly simulate location and intensity variations in water depth. However, further validation is needed in basins with different characteristics and with more available data to quantify how much error is due to inaccuracies in the boundary datasets compared to the model's ability or inability to capture the processes.

Acknowledgments

We thank the contributions made by two anonymous reviewers and Eng. David Brito, researcher in MARETEC. This research was funded by the following projects: tempQsim—"Evaluation and improvement of water quality models for application to temporary waters in Southern European catchments" (Contract no: EVK1-CT2002-00112).(http://www.tempqsim.net); EcoRiver—Evaluation of Ecotoxicity of Municipal and Industrial Wastewaters in the Rio Trancão Basin (LIFE01 ENV/P/0001416) (http://www.iambiente.pt/ecoriver/en/capa.html); SIMTEJO_I—"Monitorização do Estuário do Tejo e das Ribeiras na área de atendimento da SIMTEJO", supported by SIMTEJO, S.A. (www.simtejo.pt); ICREW—Improving Coastal and Recreational Waters, co-financed by the European Regional Development Fund through the Interreg IIIb programme for the Atlantic Area of Europe (www.icrew.info). Graphics in this paper were produced with the open source software "The R Project for Statistical Computing" (http://www.r-project.org/).

References

Arnold JG, Srinivasan R, Muttiah RS, Williams JR. Large-area hydrologic modeling and assessment: Part I. Model development. J Am Water Resour Assoc 1998;34(1):73–89.
Baretta JW, Ebenhöh W, Ruardij P. An overview over the European Regional Sea Ecosystem Model, a complex marine ecosystem model. Neth J Sea Res 1995;33(3/4):233–46.
Beeson PC, Martens SN, Breshears DD. Simulating overland flow following wildfire: mapping vulnerability to landscape disturbance. Hydrol Process 2001;15(15):2917–30.
Bicknell BR, Imhoff JC, Kittle JL, Donigian AS, Johanson RC. Hydrological Simulation Program–Fortran (HSPF): Users Manual for Release 10. Athens, Georgia: U.S. EPA Environmental Research Laboratory; 1993.
Borah DK, Bera M. Watershed-scale hydrologic and nonpoint-source pollution models: Review of applications. Trans ASABE 2004;47(3):789–803.
Braunschweig F, Chambel P, Fernandes L, Pina P, Neves R. The object oriented design of the integrated modelling system MOHID. Proceedings of the XVth International Conference on Computational Methods in Water Resources (CMWR XV), June 13–17, Chapel Hill, NC, USA; 2004.
Braunschweig F, Fernandes L, Galvão P, Trancoso R, Pina P, Neves R. MOHID GIS—A geographical information system for water modeling software. Geophysical Research Abstracts, EGU Meeting 05-A-08213, 25–29 April, Wien, Austria; 2005.
Cancino L, Neves R. Hydrodynamic and sediment suspension modelling in estuarine systems: Part I: Description of the numerical models. J Mar Syst 1999a;22(2–3):105–16.
Cancino L, Neves R. Hydrodynamic and sediment suspension modelling in estuarine systems: Part II: Application to the Western Scheldt and Gironde estuaries. J Mar Syst 1999b;22(2–3):117–31.
Canteras JC, Juanes JA, Perez L, Koev KN. Modelling the coliforms inactivation rates in the Cartabrian Sea (Bay of Biscay) from in situ and laboratory determination of T90. Water Sci Technol 1995;32(2):37–44.
Chambel-Leitão P, Braunschweig F, Fernandes L, Neves R, Galvão P. Integration of MOHID model and tools with SWAT model. Proceedings of the 4th International SWAT Conference, July 2–6 2007; 2007.
Chow VT. Open-channel hydraulics. McGraw-Hill; 1959. 680pp.
Coelho H, Santos R. Enhanced primary production over seamounts: a numerical study. Special volume on the Atlantic Iberian Continental Margin Symposium. Thalassas 2003;19(2a):144–6.
Cole T, Wells SA. CE-QUAL-W2: A two-dimensional, laterally averaged, hydrodynamic and water quality model, version 3.2. Instruction Report EL-2000-, USA Engineering and Research Development Center. Vicksburg, MS: Waterways Experiment Station; 2003.
Emaruchi, B. (1998) A Hydrological Model for Forested Mountain Watersheds. Thesis submitted to the Faculty of Graduate Studies and Research for the Degree of Doctor of Philosophy in Environmental Systems Engineering, University of Regina, Canada.
Feddes RA, Hoff H, Bruen M, Dawson T, de Rosnay P, et al. Modeling root water uptake in hydrological and climate models. B Am Meteorol Soc 2001;82:2797–810.
Fernandes L, Saraiva S, Leitão PC, Pina P, Santos A, Braunschweig F, Neves R. Mabene Deliverable D4.3d-Code and description of the benthic biogeochemistry module—Managing benthic ecosystems in relation to physical forcing and environmental constraints. MaBenE—Managing Benthic Ecosystems in relation to physical forcing and environmental constraints; 2006. (http://www.nioo.knaw.nl/projects/mabene/).
Galvão P, Chambel-Leitão P, Neves R, Chambel P. A different approach to the modified Picard method for water flow in variably saturated media. Proceedings of the XVth International Conference on Computational Methods in Water Resources (CMWR XV), June 13–17, Chapel Hill, NC, USA; 2004.
Hounam D, Werner M. The Shuttle Radar Topography Mission (SRTM). Proceedings of ISPRS-Workshop "Sensors and Mapping from Space 1999", Hannover, Germany, CD-ROM; 1999. DEM data available in http://seamless.usgs.gov/.
Kalin L, Hantush MH. Comparative assessment of two distributed watershed models with application to a small watershed. Hydrol Process 2006;20(11):2253–465.
Martins F, Leitão P, Silva A, Neves R. 3D modelling of the Sado Estuary using a new generic vertical discretisation approach. Oceanol Acta 2001;24(1):S51–62.
Mateus, M. 2006. A process-oriented biogeochemical model for marine ecosystems: development, numerical study, and application. PhD. Instituto Superior Técnico, Lisbon, Portugal. 252 pp.
Miranda R, Braunschweig F, Leitão P, Neves R, Martins F, Santos A. MOHID 2000, A coastal integrated object oriented model. Hydraulic Engineering Software VIII. WIT Press; 2000.
Montero P, Braunschweig F, Fernandes R, Leitão P. Oil Spill Monitoring and Forecasting on the Prestige-Nassau accident. 26th AMOP Technical Seminar, Victori BC, Canada; 2003.
Neves, R., 1985. Etude Experimentale et Modelisation des Circulations Trasitoire et Residuelle dans l'Estuaire du Sado. Ph. D. Thesis, University of Liége, Belgium.
Obermann, M., 2007. Nutrient dynamics in temporary waters of Mediterranean catchments. PhD thesis. University of Hannover. March 2007.
Panday S, Huyakorn PS. A fully coupled physically-based spatially-distributed model for evaluating surface/subsurface flow. Adv Water Resour 2004;27:361–82.
Pina P, Braunschweig F, Sara iva S, Santos M, Neves R. The role of physics controlling the Eutrophication processes in estuaries. Special volume on the Atlantic Iberian Continental Margin Symposium. Thalassas 2003;19(2a):157–8.
Refsgaard JC, Storm B. MIKE SHE. In: Singh VP, editor. Computer Models of Watershed Hydrology. Highlands Park, CO: Water Resources Publications; 1995. p. 809–46.
Santos A, Martins H, Coelho H, Leitão P, Neves R. A circulation model for the European ocean margin. Appl Math Model 2002;26(5):563–82.
Sara iva S, Pina P, Martins F, Santos M, Braunschweig F, Neves R. Modelling the influence of nutrient loads on Portuguese estuaries. Hydrobiologia 2007;587:5-18.
Schaap MG, Leij FJ. Using neural networks to predict soil water retention and soil hydraulic conductivity. Soil Tillage Res 1998;47:37–42.
Trancoso AR, Sara iva S, Fernandes L, Pina P, Leitão P, Neves R. Modelling macroalgae using a 3D hydrodynamic–ecological model in a shallow, temperate estuary. Ecol Model 2005;187:232–46.
Valente F, David JS, Gash JHC. Modelling interception loss for two sparse eucalypt and pine forests in central Portugal using reformulated Rutter and Gash analytical models. J Hydrol 1997;190:141–62.
van Dijk A, Bruijnzeel LA. Modelling rainfall interception by vegetation of variable density using an adapted analytical model. Part 2. Model validation for a tropical upland mixed cropping system. J Hydrol 2001;247:239–62.
van Genuchten MT. A closed-form equation for predicting the hydraulic conductivity of unsaturated soils. Soil Sci Soc Am J 1980;44:892–8.
Vieira JHL. Conditions governing the use of approximations for the Saint-Vénant equations for shallow surface water flow. J. Hydrol 1983;60:43–58.
Vossen P, Meyer-Roux J. Crop monitoring and yield forecasting activities of the MARS Project. In: King D, Jones RJA, Thomasson AJ, editors. European Land Information Systems for Agro-environmental Monitoring. Luxembourg: Office for Official Publications of the European Communities; 1995. p. 11–29. EUR 16232 EN, (http://dataservice.eea.europa.eu/dataservice/metadetails.asp?id=196).
Wool TA, Ambrose RB, Martin JL. The Water Analysis Simulation Program, User Documentation for Version 6.0, Distributed by USEPA Watershed and Water Quality Modeling. Athens, GA: Technical Support Center; 2001. (http://www.epa.gov/athens/wwqtsc/html/wasp.html).
Woolhiser DA, Smith RE, Goodrich DC. KINEROS: A kinematic runoff and erosion model: Documentation and user manual. USDA Agricultural Research Service ARS-77; 1990.